16th International Conference on Greenhouse Gas Control Technologies, GHGT-16

23rd -27th October 2022, Lyon, France

Monitoring CO_2 plume migration with lab-scale ultrasonic experimental setup

Hailun Ni[a,*], Ricardo Braganca[b], Nicola Tisato[b], T. A. Meckel[a]

[a]*Bureau of Economic Geology, Jackson School of Geosciences, The University of Texas at Austin, Austin, TX 78758, USA*
[b]*Department of Geological Sciences, Jackson School of Geosciences, The University of Texas at Austin, Austin, TX 78712, USA*

Abstract

A lab-scale ultrasonic experimental setup has been constructed to detect the presence of a trapped gas plume in a reduced-scale physical analog beadpack model. By employing the same principles as used in seismic surveys, the lab-scale ultrasonic system can generate and record ultrasonic waves in a water-filled tank and detect submerged objects or two-phase fluid density differences within porous media. In this study, the experimental domain has a fine-bead anticline barrier within the coarse-bead matrix. The lab-scale ultrasonic setup is then used to scan the tank both before and after air injection. The zero offset results show that even before data processing and image inversion, the presence of the air cap is clearly recognized. Future directions for the lab-scale ultrasonic experimental setup include extending this experimental methodology to greater geological complexity as well as other surrogate fluid pairs in order to increase the accuracy of CO_2 plume monitoring in heterogeneous domains with seismic methods.

Keywords: CO_2 geologic storage; beadpack experiments; 2D ultrasonic imaging; seismic survey; multiphase flow in porous media

1. Introduction

In geologic CO_2 storage, seismic survey is an important method to monitor the CO_2 plume migration extent, detect possible subsurface leakages, and to assist with computing saturation values during the injection and the post-injection periods [1–3]. Time-lapse three-dimensional seismic surveys, or 4D seismic surveys, have been widely adopted as an effective monitoring method at various CO_2 storage sites, including Aquistore [4–6], In Salah [7,8], Ketzin [9–11], Otway [12–14], Sleipner [15,16], Snohvit [17,18], and Weyburn [19–21].

In order to increase the accuracy of CO_2 plume detection and monitoring in heterogeneous domains with such seismic methods, we built a lab-scale ultrasonic experimental setup that is capable of acquiring high-resolution two-dimensional (2D) images by applying seismic survey principles to reduced-scale physical analog models. The setup can detect heterogeneous structures through ultrasonic imaging as shown in Fig. 1. Zero offset experimental results in Fig. 1 have shown that the setup can correctly identify a brass rod submerged in water in the middle of the tank as well as the interface between water and the top of the beadpack for a water-filled packed tank. In this study, we use this setup to image two-phase fluid flow experiments conducted in an intermediate-scale beadpack to demonstrate the ability of the lab-scale ultrasonic system to detect a trapped gas plume.

* Corresponding author. *Email address:* hailun.ni@beg.utexas.edu

Electronic copy available at: https://ssrn.com/abstract=4273218

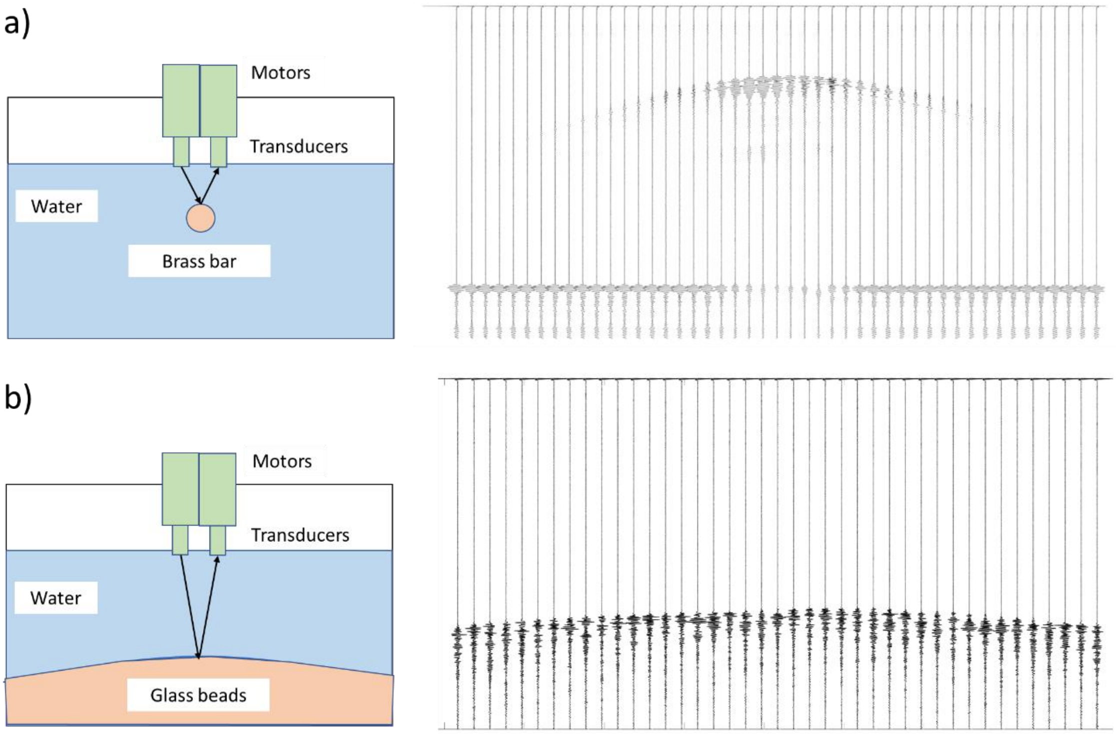

Fig. 1. Illustration of the tank configuration (left) and the corresponding acquired 2D zero offset panels (right) for a submerged brass bar (a) and water-saturated glass beads (b).

While prior literature exists on similar lab-scale ultrasonic setups [22–34], all of the prior setups were intended to image only heterogeneous structures such as different metal/resin shapes, sand/kaolin contrast, and varying glass bead types without injecting another fluid into their physical analog model domains. The only exception is that Sherlock et al. [24] used their lab-scale ultrasonic setup to construct zero offset surveys of an air cap trapped in water beneath an impermeable barrier made up of a kaolin/sand mixture. However, to the extent of the authors' knowledge, no previous attempts were made to use a lab-scale ultrasonic setup in a physical analog model to image the gas plume before and after injection, as is done in the current study.

In this work, the experiment uses the setup to detect air/water fluid density contrast in a beadpack with a simple 2D anticline geometry, similar to the experimental setup in Sherlock et al. [24]. For future experiments, we can move on to more complex geometries, and also use the heptane/glycerol+water mixture surrogate fluid pair, which has a lower density difference but is more representative of supercritical CO_2 and brine interactions at reservoir conditions.

2. Materials and methods

For the lab-scale ultrasonic system, we mount two immersion piezoelectric transducers (Olympus, 1 MHz corner frequency) on motorized gantries on a rail. Gantries move along the rail while transducers produce and acquire elastic waves in the sand tank. Thus, we produce 2D shot gathers each containing 27 traces. There are three main components in the lab-scale ultrasonic system as shown in Fig. 2. They are: a) an ultrasonic signal generation and receiving system, b) motors and their control system, and c) a sand tank and its pumping system. Component a) consists of a pulse generator (to generate source signals), an oscilloscope (to receive signals), and two transducers. Component b) consists of a rail (to mount the gantries with transducers), two motorized gantries (one for each transducer), and an ARDUINO®

Electronic copy available at: https://ssrn.com/abstract=4273218

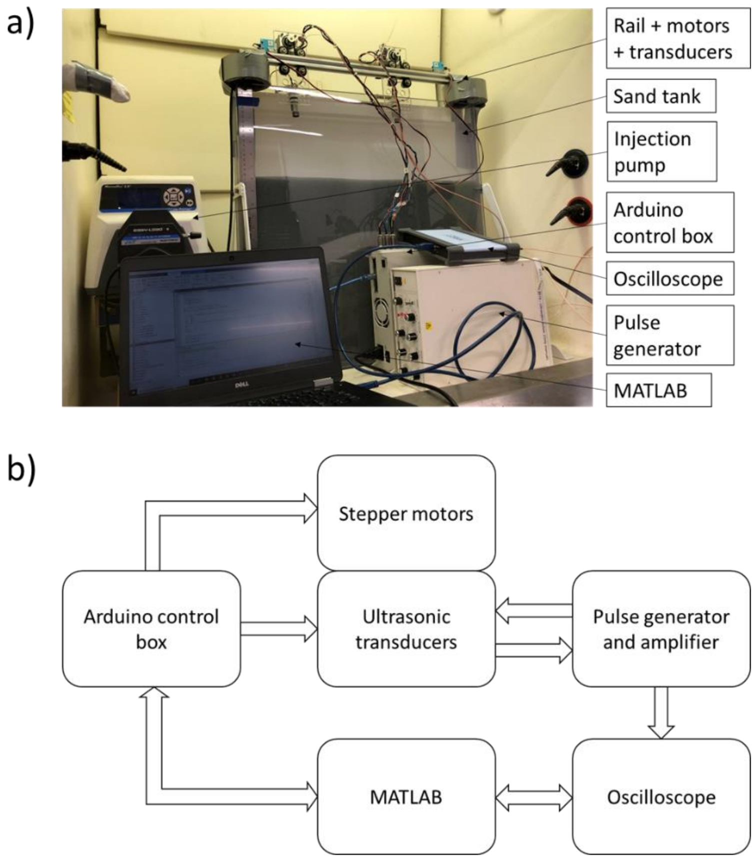

Fig. 2. Photo (a) and illustration (b) of the experimental setup for the lab-scale ultrasonic system.

control box (to command the motors). Finally, component c) includes a peristaltic pump (to inject the nonwetting phase) and a thin polycarbonate sand tank that is similar to a vertical Hele-Shaw cell so that the plume location can be visually examined.

The internal dimension of the sand tank is 60 cm × 60 cm × 4 cm as shown in Fig. 3. The sand tank is packed with two types of glass beads in order to create an anticline structure to retain the nonwetting phase fluid. The fine-bead anticline barrier is thinnest at the top, about 3.5 cm, and thickest at the sides, about 4.5 cm. The coarse bead used has a mean grain diameter of 0.689 mm and the fine bead has a mean grain diameter of around 0.160 mm [35,36]. The sand tank packing was conducted manually using the wet packing method (packing in water) to avoid trapping any air bubbles within the sediment prior to experiment. The entire beadpack is about 40 cm tall, and the water level is 55 cm tall. After the tank is packed, air is then injected into the water-saturated domain to mimic CO_2 plume buoyant migration into the domain.

As shown in Fig. 2, we use MATLAB® to communicate with both the oscilloscope and the Arduino control box in order to program the motor motions and the ultrasonic data acquisition details. For the experiment presented in this study, we acquire ultrasonic data with a signal frequency of 1MHz over the middle 27 cm-long section of the sand tank. The immersion transducers are in constant contact with water throughout data acquisition. The stepper motors used in the setup are capable of making highly accurate steps at the millimeter resolution. To acquire ultrasonic data, first we fix the location of the gantry carrying the source transducer at one end of the tank and let the gantry carrying the receiver move away from the source making 27 stops in total with 1 cm in between each stop. At each stop, the source shoots the same ultrasound signal 500 times and the receiver listens for about 1 ms after each shot to collect 10,000 samples per trace. Finally, all 500 received signals are stacked to increase signal-to-noise ratio, and the receiver gantry moves to the next stop. The source and receiver transducers can also switch roles so that even though they are

Electronic copy available at: https://ssrn.com/abstract=4273218

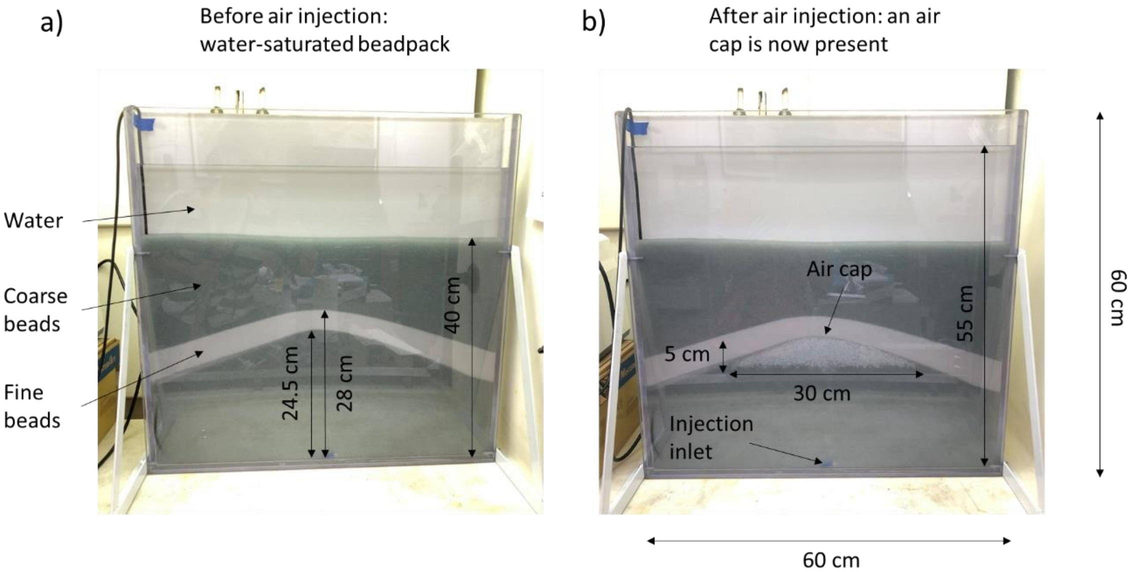

Fig. 3. Detailed beadpack configuration images showing both the water-saturated beadpack before air injection (a) and the presence of an air cap underneath the fine-bead layer after air injection (b).

mounted on a single rail, it is possible to have the source at every one of the 27 locations and the receiver at every other location. This switching step is executed inside the Arduino control box.

Two full ultrasonic scans of the beadpack domain using the aforementioned acquisition parameters were conducted, one for the water-saturated beadpack and one for the post-air-injection beadpack. The corresponding photos of the domain are shown in Fig. 3. Air is injected into the domain at 10 mL/min through a center inlet located at the bottom of the tank. Processing of the ultrasonic data acquired is the same as conventional field-scale seismic data processing. After velocity analysis, we can perform normal move-out corrections, common midpoint stacking, and post-stack migration to obtain the inverted 2D image of the sand tank [37,38]. As data processing is still ongoing, in this study, the zero offset results are presented.

3. Results and discussion

Each full ultrasonic scan takes slightly more than 5 hours to complete, and a total of 808 traces are obtained per scan (with some traces repeated). Example images of a common source gather, a common receiver gather, and a common midpoint gather are shown in Fig. 4. Next, the zero offset panels of the unprocessed data for the two scans are displayed in Fig. 5 with a zoomed-in comparison shown in Fig. 6. All these images are plotted using MATLAB codes provided by [38]. In Fig. 5, at two-way travel time (TWT) of 0.2 ms, there exists a strong reflection surface, which is the top surface of the bead pack. Multiple reflections of this surface can be observed at TWT of 0.4 and 0.6 ms, reducing in signal strength after each reflection. Elastic energy dissipates rapidly within the beadpack, which is a high attenuation material [28,39]. Therefore, the bottom of the sand tank is not clearly visible from the data for this reason.

By comparing the photos of the water-saturated beadpack and the post-air-injection beadpack in Fig. 3, we can see a clear air cap trapped underneath the fine-bead barrier. The shape of the air cap conforms to the topography of the barrier and is approximately 5 cm tall at its thickest part and 30 cm wide at the base. Because the speed of sound is different in water and in glass beads with variable degrees of water saturation, the presence of the air cap is detectable using the lab-scale ultrasonic system. This is obvious when we compare the two scans in both Fig. 5 and 6. Although the reflected ultrasonic signal is highly attenuated, both the fine-bead anticline structure and the air cap underneath are still visible in Fig. 6.

Electronic copy available at: https://ssrn.com/abstract=4273218

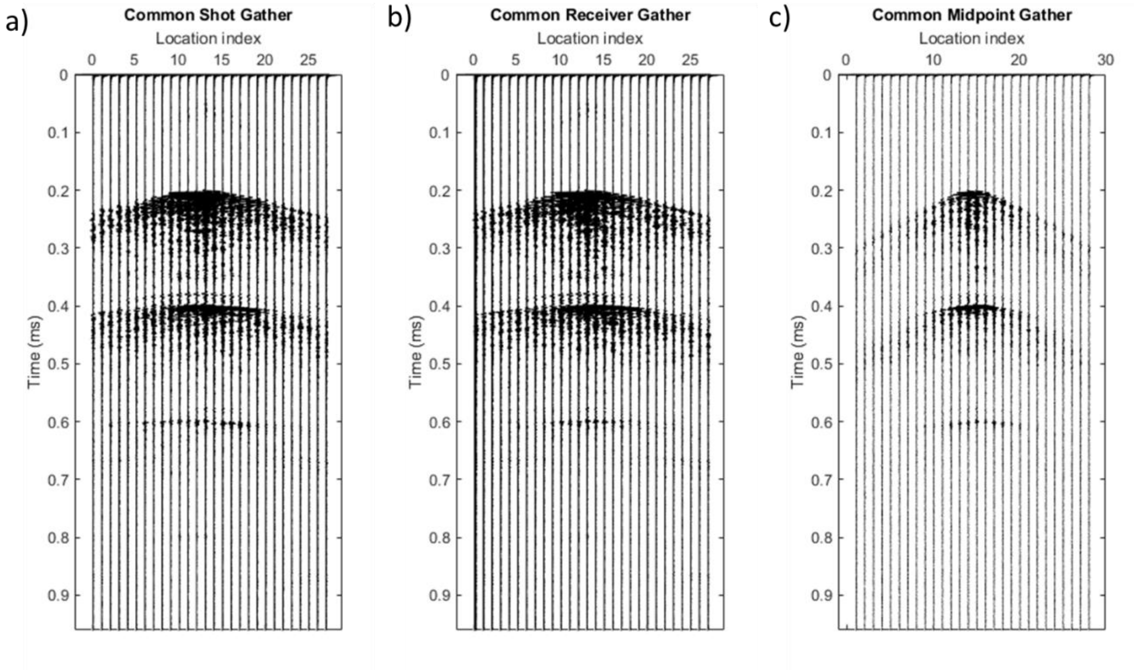

Fig. 4. a) Common shot gather for source location index 14. b) Common receiver gather for receiver location index 14. c) Common midpoint gather for midpoint location index 14. All images plotted using data from the water-saturated scan.

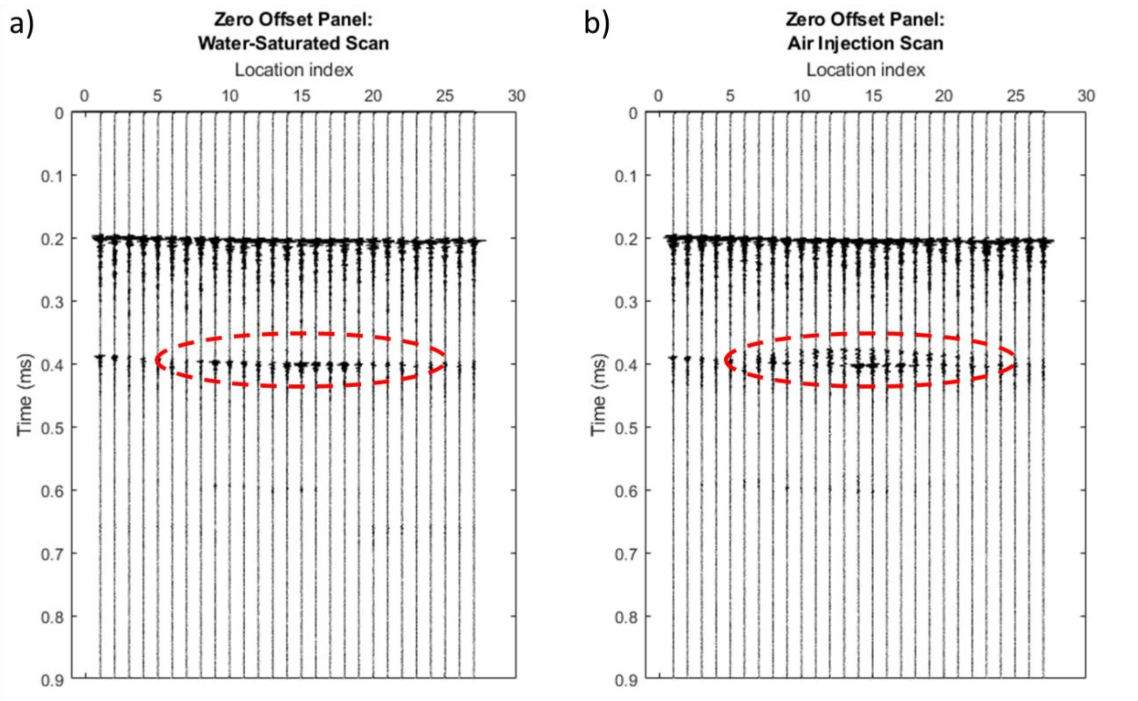

Fig. 5. Zero offset panels for the water-saturated scan (a) and the air injection scan (b). Red dashed circles highlight the area of differences between the water-saturated scan and the air injection scan (the air cap region).

Electronic copy available at: https://ssrn.com/abstract=4273218

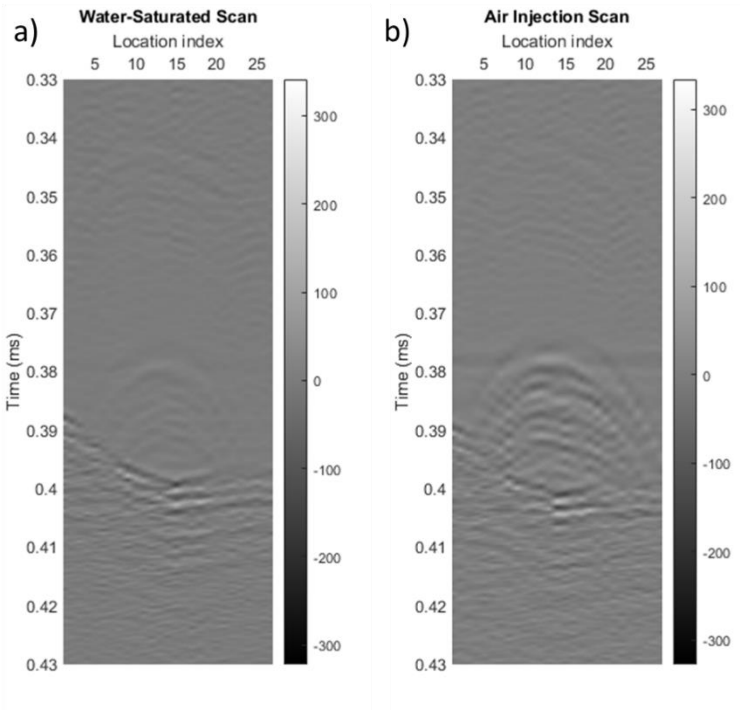

Fig. 6. Grey variable density display of the zero offset panels for both the water-saturated scan (a) and the air injection scan (b) zoomed into the air cap region.

4. Conclusions

In this study, we presented a lab-scale ultrasonic system that is capable of acquiring 2D ultrasonic images of physical sand tank models. The sand tank is first packed with water-saturated glass beads containing an anticline structure. Then air is injected into the anticline structure to form a trapped air cap. The lab-scale ultrasonic system can detect the presence of the air cap. Future experiments include extending this methodology to more complex geological heterogeneity and surrogate fluid pairs with lower density/acoustic impedance differences.

Acknowledgements

This work was supported by the U.S. Department of Energy under DOE Award Number DE-FE0031558 and the Jackson School of Geosciences Equipment Committee at the University of Texas at Austin with an equipment matching award. The authors have no known financial conflicts of interest.

Disclaimer

This report was prepared as an account of work sponsored by an agency of the United States Government. Neither the United States Government nor any agency thereof, nor any of their employees, makes any warranty, express or implied, or assumes any legal liability or responsibility for the accuracy, completeness, or usefulness of any information, apparatus, product, or process disclosed, or represents that its use would not infringe privately owned rights. Reference herein to any specific commercial product, process, or service by trade name, trademark, manufacturer, or otherwise does not necessarily constitute or imply its endorsement, recommendation, or favoring by

Electronic copy available at: https://ssrn.com/abstract=4273218

the United States Government or any agency thereof. The views and opinions of authors expressed herein do not necessarily state or reflect those of the United States Government or any agency thereof.

References

[1] Z. Wang, W.P. Harbert, R.M. Dilmore, L. Huang, Modeling of time-lapse seismic monitoring using CO2 leakage simulations for a model CO2 storage site with realistic geology: Application in assessment of early leak-detection capabilities, Int. J. Greenh. Gas Control. 76 (2018) 39–52. https://doi.org/10.1016/j.ijggc.2018.06.011.

[2] D. Lumley, 4D seismic monitoring of CO2 sequestration, Lead. Edge. 29 (2010) 150–155. https://doi.org/10.1190/1.3304817.

[3] R.A. Chadwick, B.P. Marchant, G.A. Williams, CO2 storage monitoring: Leakage detection and measurement in subsurface volumes from 3D seismic data at Sleipner, Energy Procedia. 63 (2014) 4224–4239. https://doi.org/10.1016/j.egypro.2014.11.458.

[4] D.J. White, L.A.N. Roach, B. Roberts, T.M. Daley, Initial results from seismic monitoring at the aquistore CO2 storage site, Saskatchewan, Canada, Energy Procedia. 63 (2014) 4418–4423. https://doi.org/10.1016/j.egypro.2014.11.477.

[5] D.J. White, L.A.N. Roach, B. Roberts, Time-lapse seismic performance of a sparse permanent array: Experience from the aquistore CO2 storage site, Geophysics. 80 (2015) WA35–WA48. https://doi.org/10.1190/GEO2014-0239.1.

[6] L.A.N. Roach, D.J. White, B. Roberts, Assessment of 4D seismic repeatability and CO2 detection limits using a sparse permanent land array at the Aquistore CO2 storage site, Geophysics. 80 (2015) WA1–WA13. https://doi.org/10.1190/GEO2014-0201.1.

[7] P.S. Ringrose, A.S. Mathieson, I.W. Wright, F. Selama, O. Hansen, R. Bissell, N. Saoula, J. Midgley, The in salah CO2 storage project: Lessons learned and knowledge transfer, Energy Procedia. 37 (2013) 6226–6236. https://doi.org/10.1016/j.egypro.2013.06.551.

[8] A. Mathieson, J. Midgley, K. Dodds, I. Wright, P. Ringrose, N. Saoul, CO2 sequestration monitoring and verification technologies applied at Krechba, Algeria, Lead. Edge. 29 (2010) 216–222. https://doi.org/10.1190/1.3304827.

[9] S. Lüth, P. Bergmann, F. Huang, M. Ivandic, A. Ivanova, C. Juhlin, T. Kempka, 4D Seismic Monitoring of CO2 Storage during Injection and Post-closure at the Ketzin Pilot Site, Energy Procedia. 114 (2017) 5761–5767. https://doi.org/10.1016/j.egypro.2017.03.1714.

[10] M. Ivandic, C. Yang, S. Lüth, C. Cosma, C. Juhlin, Time-lapse analysis of sparse 3D seismic data from the CO2 storage pilot site at Ketzin, Germany, J. Appl. Geophys. 84 (2012) 14–28. https://doi.org/10.1016/j.jappgeo.2012.05.010.

[11] A. Ivanova, A. Kashubin, N. Juhojuntti, J. Kummerow, J. Henninges, C. Juhlin, S. Lüth, M. Ivandic, Monitoring and volumetric estimation of injected CO 2 using 4D seismic, petrophysical data, core measurements and well logging: A case study at Ketzin, Germany, Geophys. Prospect. 60 (2012) 957–973. https://doi.org/10.1111/j.1365-2478.2012.01045.x.

[12] M. Urosevic, R. Pevzner, A. Kepic, P. Wisman, V. Shulakova, S. Sharma, Time-lapse seismic monitoring of CO2 injection into a depleted gas reservoir—Naylor Field, Australia, Lead. Edge. 29 (2010) 164–169. https://doi.org/10.1190/1.3304819.

[13] R. Pevzner, M. Urosevic, E. Caspari, R.J. Galvin, M. Madadi, T. Dance, V. Shulakova, B. Gurevich, V. Tcheverda, Y. Cinar, Feasibility of time-lapse seismic methodology for monitoring the injection of small quantities of CO2 into a saline formation, CO2CRC otway project, Energy Procedia. 37 (2013) 4336–4343. https://doi.org/10.1016/j.egypro.2013.06.336.

[14] R. Pevzner, V. Shulakova, A. Kepic, M. Urosevic, Repeatability analysis of land time-lapse seismic data: CO2CRC Otway pilot project case study, Geophys. Prospect. 59 (2011) 66–77. https://doi.org/10.1111/j.1365-2478.2010.00907.x.

[15] R.A. CHADWICK, R. ARTS, O. EIKEN, 4D seismic quantification of a growing CO 2 plume at Sleipner, North Sea, Geol. Soc. London, Pet. Geol. Conf. Ser. 6 (2005) 1385–1399. https://doi.org/10.1144/0061385.

[16] T.A. Torp, J. Gale, Demonstrating storage of CO2 in geological reservoirs: The Sleipner and SACS projects,

Electronic copy available at: https://ssrn.com/abstract=4273218

Energy. 29 (2004) 1361–1369. https://doi.org/10.1016/j.energy.2004.03.104.
[17] O. Eiken, P. Ringrose, C. Hermanrud, B. Nazarian, T.A. Torp, L. Høier, Lessons Learned from 14 years of CCS Operations: Sleipner, In Salah and Snøhvit, Energy Procedia. 4 (2011) 5541–5548. https://doi.org/10.1016/j.egypro.2011.02.541.
[18] T. Maldal, I.M. Tappel, CO2 underground storage for Snøhvit gas field development, Energy. 29 (2004) 1403–1411. https://doi.org/10.1016/j.energy.2004.03.074.
[19] T.L. Davis, M.J. Terrell, R.D. Benson, R. Cardona, R.R. Kendall, R. Winarsky, Multicomponent seismic characterization and monitoring of the CO2 flood at Weyburn Field, Saskatchewan, Lead. Edge. 22 (2003) 696–697. https://doi.org/10.1190/1.1599699.
[20] G. Li, 4D seismic monitoring of CO2 flood in a thin fractured carbonate reservoir, Lead. Edge (Tulsa, OK). 22 (2003) 690–695. https://doi.org/10.1190/1.1599698.
[21] D.J. White, G. Burrowes, T. Davis, Z. Hajnal, K. Hirsche, I. Hutcheon, E. Majer, B. Rostron, S. Whittaker, Greenhouse gas sequestration in abandoned oil reservoirs: The International Energy Agency Weyburn pilot project, GSA Today. 14 (2004) 4–10. https://doi.org/10.1130/1052-5173(2004)014<004:GGSIAO>2.0.CO;2.
[22] P. Bergamo, L. Bodet, L.V. Socco, R. Mourgues, V. Tournat, Physical modelling of a surface-wave survey over a laterally varying granular medium with property contrasts and velocity gradients, Geophys. J. Int. 197 (2014) 233–247. https://doi.org/10.1093/gji/ggt521.
[23] L. Bodet, A. Dhemaied, R. Martin, R. Mourgues, F. Rejiba, V. Tournat, Small-scale physical modeling of seismic-wave propagation using unconsolidated granular media, Geophysics. 79 (2014) T323–T339. https://doi.org/10.1190/GEO2014-0129.1.
[24] D.H. Sherlock, J.A. McDonald, B.J. Evans, Seismic imaging of sandbox models, 1997 SEG Annu. Meet. (1997) 1371–1374. https://doi.org/10.1190/1.1885661.
[25] B. Solymosi, N. Favretto-Cristini, V. Monteiller, P. Cristini, B. Ursin, D. Komatitsch, Seismic surveying and imaging at the laboratory scale: A framework to cross-validate experiments and simulations for a salt-body environment, Geophysics. 85 (2020) T123–T139. https://doi.org/10.1190/geo2019-0313.1.
[26] R. Valensi, D. Leparoux, O. Durand, F. Bretaudeau, R. Brossier, P. Côte, Quantitative imagery of shallow structures with multicomponent: Full waveform inversion and physical scale modeling, Near Surf. Geosci. 2012. (2012) 3–5. https://doi.org/10.3997/2214-4609.20143326.
[27] F. Bretaudeau, D. Leparoux, O. Durand, O. Abraham, Small-scale modeling of onshore seismic experiment: A tool to validate numerical modeling and seismic imaging methods, Geophysics. 76 (2011). https://doi.org/10.1190/geo2010-0339.1.
[28] M.-L. Buddensiek, Seismic imaging of sandbox models, 2009. https://doi.org/10.17169/refubium-4670.
[29] N. Favretto-Cristini, B. Solymosi, V. Monteiller, P. Cristini, B. Ursin, Reduced-scale lab experiments : a valuable tool for exploring current challenges of seismic surveying, modeling and imaging in complex marine environments at a low cost and in an agile way ?, in: Forum Acusticum, Lyon, France, 2020: pp. 2125–2132. https://doi.org/https://dx.doi.org/10.48465/fa.2020.0330.
[30] C.M. Krawczyk, M.L. Buddensiek, O. Oncken, N. Kukowski, Seismic imaging of sandbox experiments-laboratory hardware setup and first reflection seismic sections, Solid Earth. 4 (2013) 93–104. https://doi.org/10.5194/se-4-93-2013.
[31] C.M. Krawczyk, M.L. Buddensiek, J. Philipp, N. Kukowski, O. Oncken, Midget seismic in sandbox models - Hardware setup and first data generation, 69th Eur. Assoc. Geosci. Eng. Conf. Exhib. 2007 Secur. Futur. Inc. SPE Eur. 2007. 2 (2007) 1123–1127. https://doi.org/10.3997/2214-4609.201401621.
[32] Y. Mo, S.A. Greenhalgh, J.O.A. Robertsson, H. Karaman, The development and testing of a 2D laboratory seismic modelling system for heterogeneous structure investigations, J. Appl. Geophys. 116 (2015) 224–235. https://doi.org/10.1016/j.jappgeo.2015.03.014.
[33] D. Pageot, D. Leparoux, O. Durand, M. Le Feuvre, P. Côte, Y. Capdeville, Refined experimental studies for improving the reduced-scale physical modeling of seismic subsurface measurement, Near Surf. Geosci. 2015 - 21st Eur. Meet. Environ. Eng. Geophys. (2015) 496–500. https://doi.org/10.3997/2214-4609.201413763.
[34] S. Pasquet, L. Bodet, P. Bergamo, R. Guérin, R. Martin, R. Mourgues, V. Tournat, Small-Scale Seismic Monitoring of Varying Water Levels in Granular Media, Vadose Zo. J. 15 (2016) vzj2015.11.0142. https://doi.org/10.2136/vzj2015.11.0142.

Electronic copy available at: https://ssrn.com/abstract=4273218

[35] P.G. Krishnamurthy, T.A. Meckel, D. DiCarlo, Mimicking Geologic Depositional Fabrics for Multiphase Flow Experiments, Water Resour. Res. 55 (2019) 9623–9638. https://doi.org/10.1029/2019WR025664.
[36] H. Ni, T.A. Meckel, Characterizing the Effect of Capillary Heterogeneity on Multiphase Flow Pulsation in an Intermediate-Scale Beadpack Experiment Using Time Series Clustering and Frequency Analysis, Water Resour. Res. 57 (2021) 1–17. https://doi.org/10.1029/2021WR030876.
[37] W. Ashcroft, A petroleum geologist's guide to seismic reflection, John Wiley & Sons, 2011.
[38] W.A. Mousa, A.A. Al-Shuhail, Processing of Seismic Reflection Data Using MATLAB™, Synth. Lect. Signal Process. 5 (2011) 1–97. https://doi.org/10.2200/S00384ED1V01Y201109SPR010.
[39] G.W. Purnell, Observations of wave velocity and attenuation in two-phase media., Geophysics. 51 (1986) 2193–2199. https://doi.org/10.1190/1.1442072.

Electronic copy available at: https://ssrn.com/abstract=4273218